Electronic structure of ZnO nanorods studied by angle-dependent x-ray absorption spectroscopy and scanning photoelectron microscopy

J. W. Chiou, J. C. Jan, H. M. Tsai, C. W. Bao, and W. F. Pong[a)]
Department of Physics, Tamkang University, Tamsui, Taiwan 251, Republic of China

M.-H. Tsai
Department of Physics, National Sun Yat-Sen University, Kaohsiung, Taiwan 804, Republic of China

I.-H. Hong,[b)] R. Klauser, and J. F. Lee
National Synchrotron Radiation Research Center, Hsinchu, Taiwan 300, Republic of China

J. J. Wu and S. C. Liu
Department of Chemical Engineering, National Cheng Kung University, Tainan, Taiwan 600, Republic of China

(Received 8 December 2003; accepted 12 March 2004; published online 20 April 2004)

Angle-dependent x-ray absorption near-edge structure (XANES) and scanning photoelectron microscopy measurements were performed to differentiate local electronic structures at the tips and sidewalls of highly aligned ZnO nanorods. The overall intensity of the O *K*-edge XANES spectra is greatly enhanced for small photon incident angles. In contrast, the overall intensity of the Zn *K*-edge XANES is much less sensitive to the photon incident angle. Both valence-band photoemission and O *K*-edge XANES spectra show substantial enhancement of O 2*p* derived states near the valence band maximum and conduction band minimum, respectively. The spatially resolved Zn 3*d* core level spectra from tip and sidewall regions show the lack of chemical shift. All the results consistently suggest that the tip surfaces of the highly aligned ZnO nanorods are terminated by O ions and the nanorods are oriented in the [0001] direction. © *2004 American Institute of Physics.* [DOI: 10.1063/1.1737075]

Nanoscale materials, particles with sizes in the order of nanometer, have recently been the subjects of intense research.[1] The interest arises from the fact that the electronic structures of these materials differ from those of the bulk materials.[2] The availability of nanorods and nanowires enables fundamental studies of one-dimensional electronic systems and the fabrications of optoelectronic nanodevices.[3] Zinc oxide (ZnO) is a potentially important material because of its electrical and optoelectronic characteristics.[4] UV lasing at room temperature was recently observed in highly oriented ZnO nanorod arrays.[5] Polarization-dependent O *K*-edge x-ray absorption and first-principles theoretical calculation were performed on highly oriented ZnO microrods.[6] In this study, angle-dependent x-ray absorption near-edge structure (XANES) at the O *K*, Zn L_3 and *K* edges and scanning photoelectron microscopy (SPEM) measurements were performed to understand details of the electronic structures of highly oriented ZnO nanorods.

Angle-dependent O *K*-, Zn L_3- and *K*-edge XANES measurements were taken at the high-energy spherical grating monochromator and wiggler-C beamlines by the fluorescence mode, respectively, and SPEM measurements were performed at the U5-undulator beamline of the National Synchrotron Radiation Research Center (NSRRC) in Hsinchu, Taiwan. In the angle-dependent XANES measurements, the direction of the electric polarization vector was varied with respect to the orientation of the ZnO nanorods and spectra were obtained for angles from 10°–70° or 80° between the direction of the incident photon and the orientation of the nanorods. The SPEM-end station at NSRRC has been described elsewhere.[7] Highly oriented ZnO nanorods were prepared on Si(100) substrate using catalyst-free chemical vapor deposition method at low temperature. Details of the preparation and characterization of the ZnO nanorods can be found elsewhere.[8] Scanning electron microscope (SEM) and transmission electron microscope (TEM) measurements revealed that ZnO nanorods were ~250 nm long and ~45 nm in diameter and exhibited a hexagonal (wurtzite) structure with the rods oriented in the *c*-axis direction as displayed in Figs. 1(a) and 1(b), respectively.

Figures 2 and 3 plot the angle-dependent XANES spectra of highly oriented ZnO nanorods at the O and Zn *K* edges, respectively. The upper inset in Fig. 2 shows the incident angle θ relative to the orientation of the nanorods. Variation of the absorption intensity of the O and Zn *K*-edge XANES spectra with respect to the incident angle has been regarded as evidence of anisotropy in O and Zn *p* states, respectively, which are also present in ZnO microrods[6] and thin films.[9] The variation in the general line shape and the positions of the peaks of the O and Zn *K*-edge XANES spectra of the ZnO nanorods with respect to the photon incident angle are similar to those observed previously in the N and Ga *K*-edge XANES spectra of the GaN thin film,[10] due to the same crystal structure and similar lattice constants. Note that the lattice constants of ZnO are $a=3.25$ Å and $c=5.20$ Å and of GaN are $a=3.19$ Å and $c=5.19$ Å.

According to the dipole-transition selection rule, features

a)Author to whom correspondence should be addressed; electronic mail: wfpong@mail.tku.edu.tw
b)Permanent address: Department of Applied Physics, National Chiayi University, Chiayi 600, Taiwan, Republic of China.

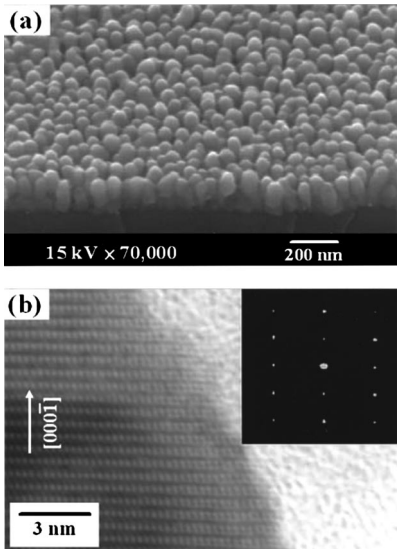

FIG. 1. (a) SEM image and (b) high-resolution TEM image and its corresponding electron diffraction (inset) of the ZnO nanorods.

A_1-G_1 (Fig. 2) and A_2-G_2 (Fig. 3) can be attributed to O $2p$ and Zn $4p$ derived states, respectively. Møller, Komolov, and Lazneva[11] calculated O and Zn derived p partial densities of states for bulk ZnO and obtained four features in the unoccupied energy bands. The present O and Zn *K*-edge XANES spectra of the ZnO nanorods are more complicated. There are two factors that give rise to the angle dependence of the spectra upon the incident angle of the photons. One is due to asymmetry in the orientations of the σ bonds (bilayer bonds) and the π bond (*c*-axis bond). The bilayer bonds lie approximately perpendicular to the *c* axis, while the *c*-axis bond lies parallel to the *c* axis. Thus, bilayer- and *c*-axis-bond states are preferentially probed at small and large incidence angles, respectively, because the polarization of the photons is parallel to the bilayer and the *c* axis bonds at the respective incident angles.[10] Another is due to the arrangement of the highly aligned nanorods; the spectra obtained at normal incidence ($\theta=0°$) is expected to be dominated by contributions from the tip area, whereas at large incident angle ($\theta=70°$) it should have mainly contributions from the sidewalls of the ZnO nanorods.[12] The results presented in Fig. 2 indicate that features A_1, B_1, and D_1 increase substantially in intensity, especially feature B_1, but remain approximately at the same position when the incident angle decreases. Feature C_1 shifts slightly to higher energy, while features F_1 and G_1 increase substantially in intensity and approach each other when the incident angle decreases. Only the intensity of feature E_1 is reduced with smaller incident angle. Since most of the features are enhanced in the tip region, the bilayer- and *c*-axis-bond contributions cannot be distinguished. Overall, the intensity of the tip spectrum is greatly enhanced relative to that of the sidewall spectrum. On the other hand, in the Zn *K*-edge spectra features A_2, D_2, E_2, F_2, and G_2 are relatively insensitive to the incident angle (Fig. 3). Features B_2 and C_2 merge into one single feature at small incident angle corresponding to the tip region. The overall or integrated intensity of the Zn *K*-edge tip spectrum does not differ significantly from that of the sidewall spectrum. The variation of the intensities of the O and Zn *K*-edge spectra show that the local electronic structure at the O ions in the tip region is very different from those in the sidewall region, while the local electronic structures at the Zn ions differ much less significantly between tip and sidewall. These results suggest that the tip surfaces are terminated by O ions and not by Zn ions.

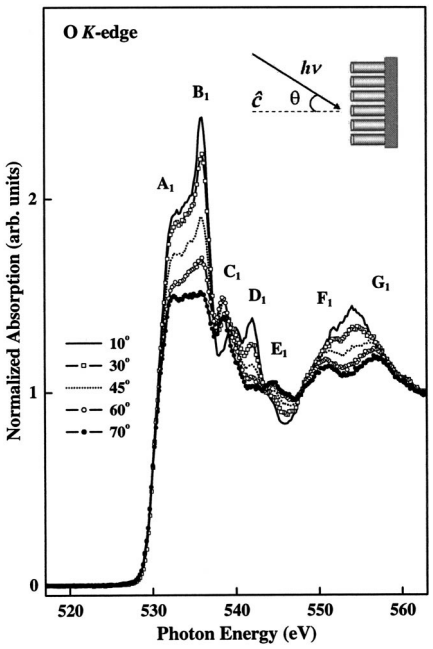

FIG. 2. The O *K*-edge XANES spectra of ZnO nanorods for various photon incident angles. The inset defines the photon incident angle.

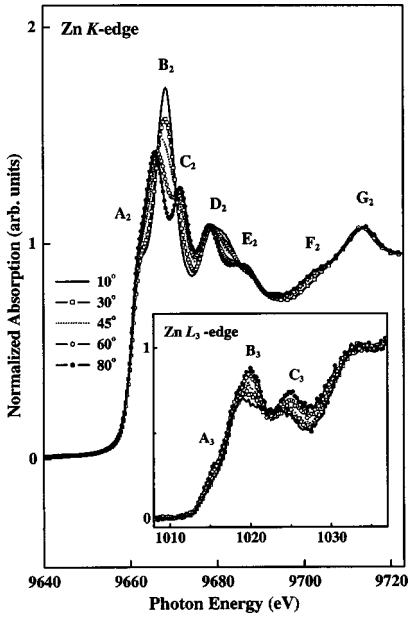

FIG. 3. The Zn *K*-edge XANES spectra of ZnO nanorods for various photon incident angles. The inset plots the Zn L_3-edge XANES spectra.

The inset of Fig. 3 plots the angle dependent Zn L_3-edge XANES spectra of the ZnO nanorods. According to the dipole-transition selection rule, Zn L_3-edge XANES probes the unoccupied Zn *s*- and *d*-derived states. The Zn $3d$ orbital is fully occupied, so the lowest unoccupied orbital of the Zn ion is Zn $4s$, followed by Zn $4p$ and $4d$. The inset in Fig. 3 reveals that the position of feature A_3 is less sensitive to the photon incident angle, while those of features B_3 and C_3

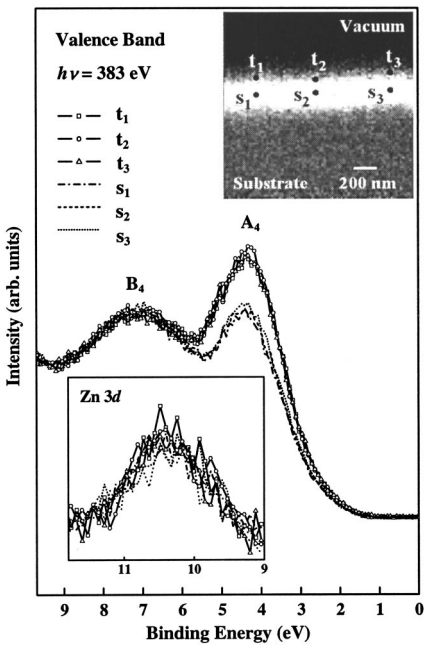

FIG. 4. Valence-band SPEM spectra obtained from regions marked by t_1-t_3 and s_1-s_3 shown in the upper inset, which displays SPEM Zn $3d$ cross-sectional image of ZnO nanorods. The lower inset shows the Zn $3d$ core-level photoemission spectra from regions t_1-t_3 and s_1-s_3, respectively.

shift significantly to lower energies when the photon incident angle is decreased. This trend implies that feature A_3 has contributions from Zn $4s$ derived states, which is not sensitive to the photon incident angle, while features B_3 and C_3 are dominated by *d*-like states, which are highly directional. Furthermore, the intensities of all features A_3, B_3, and C_3 decrease as θ decreases, which indicate that the number of unoccupied Zn $4s$ and $4d$ states near the conduction band minimum (CBM) is reduced in the tip region.

Figure 4 displays spatially resolved valence-band photoemission spectra of ZnO nanorods at various positions. The upper and lower insets in the figure also show, respectively, the Zn $3d$ SPEM cross-sectional image and core-level photoemission spectra of the aligned nanorods. The bright area in the SPEM image corresponds to the ZnO nanorods with maximum Zn $3d$ intensity. The spectra in Fig. 4 are photoelectron yields from regions marked as t_1-t_3 and s_1-s_3 shown in the upper inset, which refer to tip and sidewall regions of the nanorods. The zero energy is chosen at the Fermi level, E_f, which is the threshold of the emission spectrum. The general line shapes of the valence-band SPEM spectra of the nanorods in Fig. 4 are similar to those obtained previously from photoemission measurements of bulk ZnO.[13–15] Figure 4 obviously indicates that the intensity of feature A_4 in the valence-band SPEM spectra of the tips is apparently larger than that of feature A_4 in the spectra of the sidewalls. In contrast, the intensities of tip and sidewall B_4 features are almost the same. Since the occupied states near E_f, i.e., the valence-band maximum (VBM), are dominated by the dangling-bond states and anion derived *p* states, i.e., O $2p$ states in the present case, feature A_4 in the tip region is due to either enhanced O $2p$ states or dangling-bond states. Since feature B_4 is deep in the valence band, it can be attributed to the O $2p$ and Zn $4sp$ and $3d$ hybridized states.[14,16] The lower inset in the figure shows that the tips have the same Zn $3d$ core-level intensity and binding energy as the sidewalls, which indicates that the local environment of Zn ions is similar in the tip and sidewall regions. The lack of chemical shift of the Zn core level and the similar B_4 features in the tip and sidewall regions suggest that tip surfaces of the nanorods are not terminated by Zn ions. These results imply that the enhancement of feature A_4 in the tip region is dominantly contributed by the near-E_f valence and dangling-bond $2p$ states of O ions, which terminate the tip surfaces.

The TEM image shown in Fig. 1(b) indicates that the nanorods are either oriented in the $[0001]$ or $[000\bar{1}]$ direction. The tip surface is terminated by Zn and O, respectively, for $[0001]$ and $[000\bar{1}]$ orientations.[14,17] Our O *K*-edge XANES and valence-band SPEM spectra show that in the tip region near-VBM occupied and near-CBM unoccupied O $2p$ derived states are substantially enhanced. This can be interpreted as the narrowing of the O $2p$ derived band in the tip region relative to that in the sidewall region, which can be correlated with the reduction of the number of Zn ions that are bonded to the O ions. In other words, the tip surface is terminated by O ions and the ZnO nanorods are oriented in the $[000\bar{1}]$ direction consistent with the observations from Zn $3d$ core level and valence-band photoemission SPEM spectra.

One of the authors (W.F.P.) would like to thank the National Science Council of R.O.C. for financially supporting this research under Contract No. NSC 92-2112-M-032-025.

[1] R. W. Siegel, Phys. Today **46**, 64 (1993).
[2] J. W. Chiou, J. C. Jan, H. M. Tsai, W. F. Pong, M.-H. Tsai, I.-H. Hong, R. Klauser, J. F. Lee, C. W. Hsu, H. M. Lin, C. C. Chen, C. H. Shen, L. C. Chen, and K. H. Chen, Appl. Phys. Lett. **82**, 3949 (2003).
[3] C. M. Lieber, Solid State Commun. **107**, 607 (1998).
[4] F. Quaranta, A. Valentini, F. R. Rizzi, and G. Gasamassima, J. Appl. Phys. **74**, 244 (1993); D. M. Bagnall, Y. F. Chen, Z. Zhu, T. Yao, S. Koyama, M. Y. Shen, and T. Goto, *ibid.* **70**, 2230 (1997).
[5] M. H. Huang, S. Mao, H. Feick, H. Yan, Y. Wu, H. Kind, E. Weber, R. Russo, and P. Yang, Science **292**, 1897 (2001).
[6] J. H. Guo, L. Vayssieres, C. Persson, R. Ahuja, B. Johansson, and J. Nordgren, J. Phys. Condens. Matter **14**, 6969 (2002).
[7] R. Klauser, I.-H. Hong, T.-H. Lee, G.-C. Yin, D.-H. Wei, K.-L. Tsang, T. J. Chuang, S.-C. Wang, S. Gwo, M. Zharnikov, and J.-D. Liao, Surf. Rev. Lett. **9**, 213 (2002).
[8] J. J. Wu and S. C. Liu, Adv. Mater. (Weinheim, Ger.) **14**, 215 (2002); J. Phys. Chem. B **106**, 9546 (2002).
[9] E. Y. M. Lee, N. Tran, J. Russell, and R. N. Lamb, J. Appl. Phys. **92**, 2996 (2002).
[10] J. W. Chiou, S. Mookerjee, K. V. R. Rao, J. C. Jan, H. M. Tsai, K. Asokan, W. F. Pong, F. Z. Chien, M.-H. Tsai, Y. K. Chang, Y. Y. Chen, J. F. Lee, C. C. Lee, and G. C. Chi, Appl. Phys. Lett. **81**, 3389 (2002).
[11] P. J. Møller, S. A. Komolov, and E. F. Lazneva, J. Phys.: Condens. Matter **11**, 9581 (1999).
[12] J. W. Chiou, C. L. Yueh, J. C. Jan, H. M. Tsai, W. F. Pong, I.-H. Hong, R. Klauser, M.-H. Tsai, Y. K. Chang, Y. Y. Chen, C. T. Wu, K. H. Chen, S. L. Wei, C. Y. Wen, L. C. Chen, and T. J. Chuang, Appl. Phys. Lett. **81**, 4189 (2002).
[13] L. Ley, R. A. Pollak, F. R. McFeely, S. P. Kowalczyk, and D. A. Shirley, Phys. Rev. B **9**, 600 (1974).
[14] W. Göpel, J. Pollmann, I. Ivanov, and B. Reihl, Phys. Rev. B **26**, 3144 (1982).
[15] R. T. Girard, O. Tjernberg, G. Chiaia, S. Söderholm, U. O. Karlsson, C. Wigren, H. Nylén, and I. Lindau, Surf. Sci. **373**, 409 (1997).
[16] P. Schröer, P. Krüger, and J. Pollmann, Phys. Rev. B **47**, 6971 (1993).
[17] A. Wander, F. Schedin, P. Steadman, A. Norris, R. McGrath, T. S. Turner, G. Thornton, and N. M. Harrison, Phys. Rev. Lett. **86**, 3811 (2001).